Article

Water Quality Indicators in Three Surface Hydraulic Connection Conditions in Tropical Floodplain Lakes

Miguel Ángel Salcedo, Allan Keith Cruz-Ramírez, Alberto J. Sánchez *, Nicolás Álvarez-Pliego, Rosa Florido, Violeta Ruiz-Carrera and Sara Susana Morales-Cuetos

Diagnóstico y Manejo de Humedales Tropicales, División Académica de Ciencias Biológicas, Universidad Juárez Autónoma de Tabasco, Villahermosa, Tabasco 86040, Mexico
* Correspondence: alberthoj.sanchez@gmail.com

Abstract: Water quality indicators have been tied to natural or man-made surface hydraulic connection (SHC) conditions. Among these, temporally connected lakes (TCL) are hydraulic intermediates between isolated (IL) and permanently connected lakes (PCL). Therefore, the aim of this study is to answer if water quality indicators can estimate the possible overlap between the two opposed conditions of SHC (IL and PCL) with the intermediate one (TCL) in lakes with similar modifications in the water level regulation at the basin level. Among nine water variables sampled in six lakes with the three SHC conditions mentioned, chlorophyll *a* (Chl-*a*), Secchi disk (SD), and total phosphorus (TP) were identified as quality water indicators through principal component analysis. Furthermore, said indicators were used to measure their overlap and trophic state index deviations. The Chl-*a*, SD, and TP values in TCL showed a 0.72 overlap of PCL and IL. TP surplus measured in all the lakes was meaningful in urbanized ILs and lessened in a rural lake (PCL6) with submerged rooted macrophytes. The estimated overlap of trophic indicators between TCL, IL, and PCL in this study must be verified at a global representative scale for predictive and preventive use in the conservation of tropical coastal plain lakes.

Keywords: aquatic indicators; environmental impact; overlapped indicators; physicochemical homogenization

1. Introduction

The marked spatial and temporal variation of surface hydraulic connection (SHC) leads to intra-annual fluctuations of water quality indicators, as it modifies hydrogeomorphological and biogeochemical processes in lakes in the same floodplain [1–3]. Among these processes, the water exchange and residence time are relevant, which affect both water budgets, nutrients, and phytoplankton biomass [4–7], and short-time enrichment in floodplain lakes [8,9]. Among other factors, SHC variation can be analyzed by different conditions, such as intermittency (permanently connected, temporarily connected, and isolated) and natural or man-made interconnection between the river and lakes in the floodplain.

In this regard, for temporarily connected lakes (TCL), area magnitudes, as well as the physicochemical and phytoplankton biomass variables, fluctuate widely during the annual cycle, compared to permanently connected (PCL) and isolated (IL) lakes [10–12]. Short water residence times and the variation in nutrient concentrations, phytoplankton biomass, and increased light passage in PCL depend on the inter-annual fluctuation of the water level [1,8,9,13]. In ILs, there is less water volume and the residence time of water increases [6,14]. These conditions help explain increases in nutrient concentrations and algal biomass related to eutrophication, reduced light, dominant toxic algae, and, due to human impact, the exacerbation of the trophic state [15,16]. In this context, biogeochemical processing is also strongly tied to the residence times, and the intra-annual variation of the

water level explains the differences in nutrient enrichment in the three different hydraulic connection conditions [10,13].

SHC changes in coastal plains are linked to natural geo-hydromorphological processes over medium to long terms [17]. Recently, short-term alterations in SHC and lake conservation have been associated with the construction of hydraulic infrastructure and waste from urban, agricultural, and livestock activities [18,19], which have modified the surface water drainage and natural intra-annual flow variation patterns at a watershed scale [20,21]. Nonetheless, the magnitude of hydraulic disconnection is also related to smaller spatial scales, as hydrogeomorphology in floodplain rivers and lakes is heterogeneous throughout the basin [17,22]. Aside from the spatial scales, the restricted intra-annual fluctuation in water levels [23,24] is linked with hydrological modifications, causing a loss of lateral flooding and an increase in water residence time [4,24–26]. The loss of lateral flooding, together with the increase in water residence time, help explain the almost permanent eutrophication conditions established by the temporally limited hydraulic interconnection or the isolation of the TCL and IL lakes in the drainage area under study [27,28], as has been recorded for other basins [12,13,25,29]. Along this gradient of surface connectivity, the temporally connected floodplain lakes are intra-annually isolated or interconnected, which can mean that they share the SHC of both lakes, PCL, and IL. However, the water quality indicators in TCL have been scarcely included in most of the published results [1,12,30,31].

In this context, the determination of water quality indicators linked to SHC alteration has been rarely addressed in some regions, such as Africa, South Asia, and part of North America [3]. This unawareness of the fluctuation of water quality indicators (e.g., chlorophyll *a*, Secchi disk transparency, total phosphorus, electrical conductivity, and dissolved oxygen saturation) does not allow any form of anticipating critical environmental risks due to the lack of time series data [32] or detecting the main sources of pollution and degradation of aquatic ecosystems, in some cases, of man-made recurrent modifications, such as the annual high mortality of manatees in the Grijalva Basin [33]. In this sense, different SHC conditions in lakes (PCL, TCL, and IL) help resolve hypotheses that are tied to the alterations in the variations of water quality indicators and their effects on biodiversity [1,3]. Therefore, the objective of this research was to identify which water quality indicators explain their possible overlap in floodplain lakes with three surface hydraulic connection conditions (IL, TCL, and PCL) in a hydrologically altered floodplain, understanding overlap as the measure of data of the water quality indicators that result common with respect to a reference interval according to [34]. In this context, we hypothesize that water quality indicators measured at IL and PCL overlap with TCL indicators in a floodplain with similar surface hydraulic alteration at the basin level, but with different urban and hydraulic infrastructure. Then, the overlap of water quality indicators in different conditions of SHC in lakes located in floodplains could be a predictive and preventive tool for their conservation management.

2. Materials and Methods

2.1. Study Area

The flow in the Grijalva River basin runs from the northwest highlands and discharges into the southwestern Gulf of Mexico (Figure 1). This basin, located in the humid tropic, is topographically divided into three zones [35]: highlands (>60 MASL), terraces and knolls (20 to 60 MASL), and floodplain (<20 MASL). The study area is located in this last zone. The Mezcalapa, Pichucalco-La Sierra, and Tepetitán-Chilapa are the three main rivers that drain into the floodplain in this basin, however the La Sierra River is the only river that freely drains and remains flowing, while the Mezcalapa is dammed, and both influence the study area polygon.
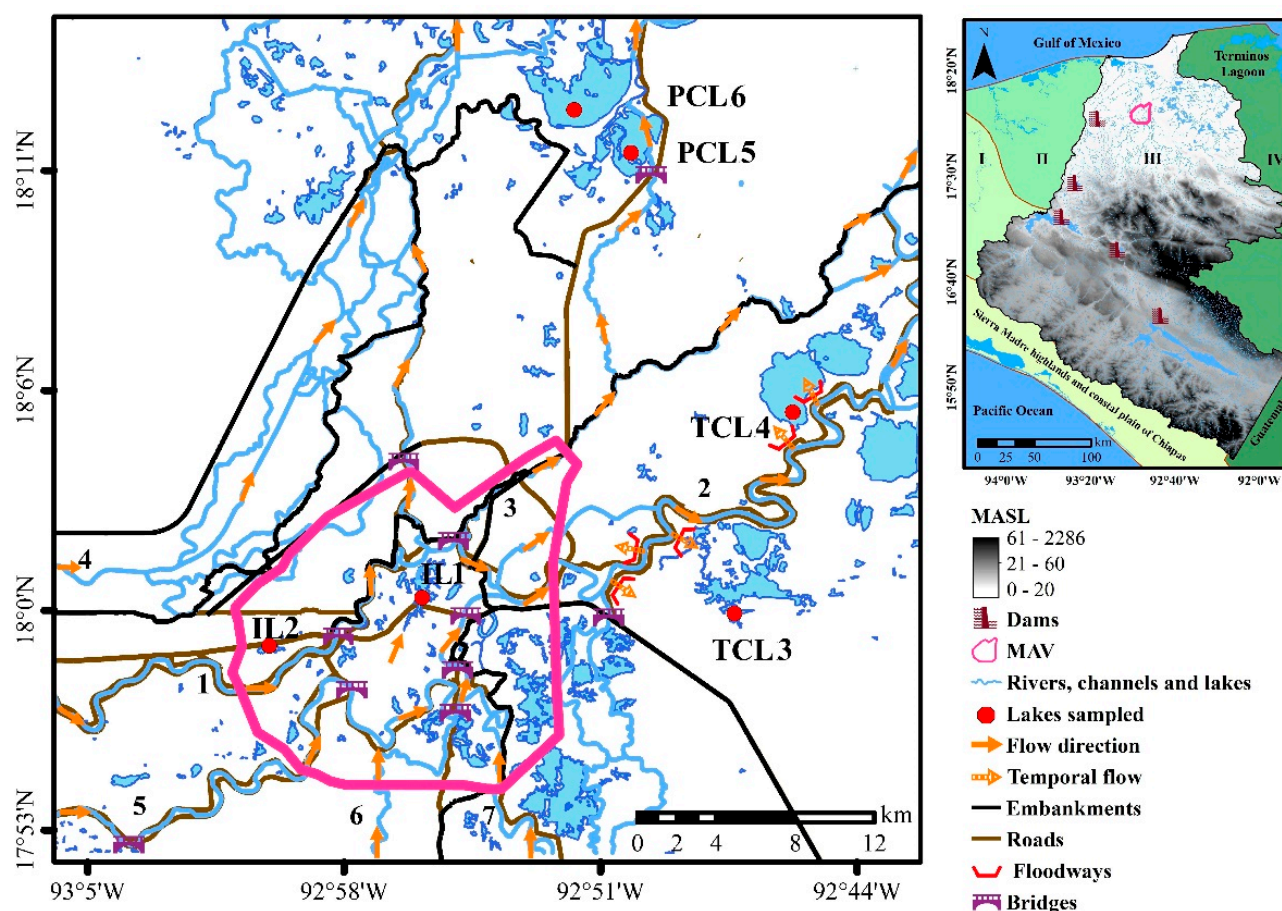
Figure 1. Location of the study area in the Grijalva River basin (III) and surrounding basins (I = Coatzacoalcos, II = Tonala, IV = Usumacinta). Distribution and configuration of lakes in the Metropolitan Area of Villahermosa (MAV) and the surrounding rural areas in the floodplain. (1) Carrizal River, (2) Grijalva River, (3) Medellin-Gonzalez River, (4) Samaria River, (5) Mezcalapa Viejo River, (6) Pichucalco River, (7) La Sierra River. IL1 = Las Ilusiones, IL2 = Loma de Caballo, TCL3 = Playa del Pozo, TCL4 = Maluco, PCL5 = Manguito, PCL6 = Pucte. MASL = meters above sea level.

The Mezcalapa River drains the Mezcalapa Viejo, Samaria, Carrizal, Medellin-Gonzalez, and Grijalva river areas. This drainage network was modified to avoid flooding the current Metropolitan Area of Villahermosa (MAV) by the construction of five banks to divert river water (16th to 20th centuries), five dams (20th century), 207 km of embankments, 56 bridges, and an added 62 h of roads (late 20th to early 21st centuries), as well as the urban sprawl that took place over the last 50 years [36,37]. The last three hydraulic transformations are key to this study, as the dams and the urban infrastructure regulate the intra-annual water level variations in two drainage areas down-river: the Mezcalapa River and the Grijalva River, and divert the flow to avoid flooding the MAV, further changing the flow magnitude and the natural flood cycle of both rivers [38–41]. These changes attributed to hydraulic and urban transformations are evidence of the alteration of wetlands in the Grijalva River floodplain [42].

Since the MAV is located in the altered study area, the MAV has an area of 20,655 ha [43] and is inhabited by 755,425 people, whereas the rural area has 115,066 inhabitants [44]. Downstream from the MAV, floodways were later built, modifying the road-embankments of the banks of the Grijalva River, and these generate temporary lateral flows into the current floodplain [36]. Agricultural, livestock, and forestry activities are also carried out in over 70% of the study area; in contrast, aquatic emergent macrophytes cover 3% of the drainage area of the Carrizal River, 6% in the Grijalva River drainage area, and 15% in the

Medellin-Gonzalez drainage area [45]. Floating aquatic plants are common in most of the lakes, the water *Eichhornia crassipes* (Mart.) Solms among them. The submerged rooted macrophyte *Vallisneria americana* Michx. was only recorded in Pucte Lake, or PCL6 [46]. In this context, the increase in population in the urban zone and the loss of hydrophytic vegetation coverage in the rural area are indications of other factors that alter the ecological conditions of the study area [18,42,46].

The six sampled lakes are located in the plain of the Grijalva River basin. The six lakes are hydraulically independent. Four are interconnected with their tributary, two PCL with the Medellin-Gonzalez and two TCL with the Grijalva Rivers, while the two IL were interconnected with the Carrizal River in the drainage area of the Río Mezcalapa (Figure 1). Of these three rivers, the Carrizal and Grijalva Rivers pass through both the MAV and the surrounding rural area, while the Medellin-Gonzalez is located down-river of the MAV (Figure 1, Table S1).

The two isolated lakes (IL) are located in the MAV. Their hydraulic isolation was established by the construction of a roadside for a highway or embankment without sewers due to urban expansion [27]. In contrast, the other four lakes include two temporally connected lakes (TCL) and two permanently connected lakes (PCL), located in the rural area, 17 to 22 km down-river of the MAV, respectively. Constructing five floodways along the roadside embankments restored the hydraulic connectivity of the two TCL during the rainy seasons [36]. Finally, the absence of urban infrastructure, combined with the construction of highways with bridges, explains the permanent hydraulic connection among the main river in PCL, the tributaries, and the lakes in the Medellin-Gonzalez River drainage area (Figure 1, Table S1).

In the Grijalva River basin plain, the Grijalva River gauge station (# 30006, El Muelle) was used as a reference for the variation in water levels on the plain of the Grijalva River basin, which varied from 1.5 to 4.9 m above sea level (MASL) on average from 2005 to 2014 and presented at least four contrasting water level conditions [47] (Figure 2).
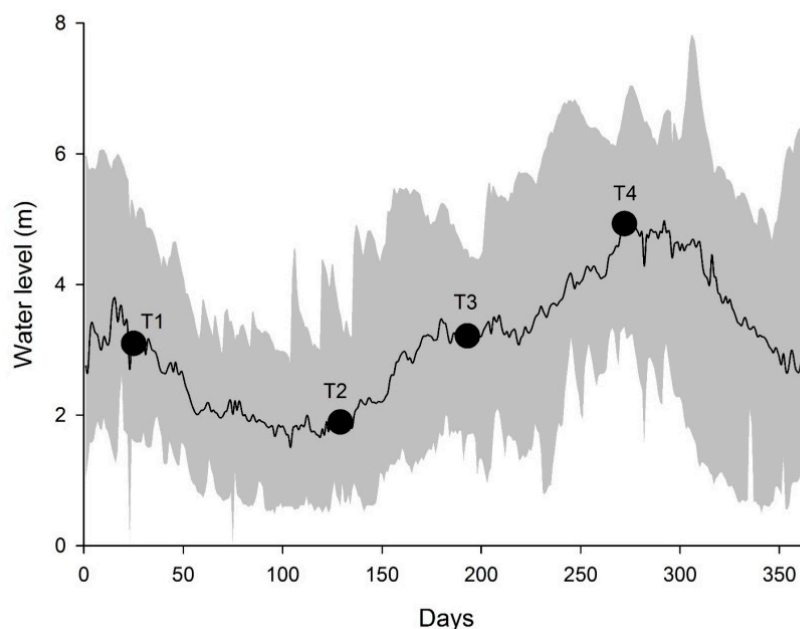
Figure 2. Daily water level variations in the Grijalva River. Water level data were taken from the hydrometric station of Las Gaviotas II, key 30,083 [47]. 4 sampling periods = black circle (T1 = transition to low level; T2 = low level; T3 = transition to high level; T4 = high level). Grey area = minimum and maximum water level. Black line = average water level (2005–2014).

2.2. Sampling

Sampling was carried out in six shallow lakes with three different surface hydraulic connections: isolated lakes, Las Ilusiones (IL1) and Loma de Caballo (IL2), temporally connected lakes, Playa del Pozo (TCL3) and Maluco (TCL4), and permanently connected lakes, Manguito (PCL5) and Pucte (PCL6) (Figure 1, Table S1). The sampling design included 3 sampling sites per lake during 4 periods (T1 = transition to low level, 20–25 January; T2 = low level, 3–9 May; T3 = transition to high level, 7–16 July; T4 = high level, 24–28 September) throughout a hydrological cycle (2013–2014), for a total of 72 samples for each of the 9 biological and physicochemical variables recorded. All samples were collected from 8:00 a.m. to 01:00 p.m. The four sampling times were established considering the expected water level changes in the Grijalva River [28,47].

According to [16,48–50], the water quality variables were quantified or measured. In situ recordings (meters) were taken for the water level (WL) using a Hondex PS-7 echo sounder (HONDA Electronics CO., LTD. Aichi, Japan) and water transparency was measured with a Secchi disk (SD). The values of dissolved oxygen saturation (DOS, %), potential hydrogen (pH), and electrical conductivity (EC, $\mu S\ cm^{-1}$), and concentrations of ammonium (NH_4^+, $mg\ L^{-1}$), nitrates (NO_3^-, $mg\ L^{-1}$), and chlorophyll a (Chl-a, $\mu g\ L^{-1}$) were estimated using a YSI 6600 V2–2 multi-parameter probe (Xylem Analytics. Queensland, Australia). Water samples were collected at mid-depth after recording the depth at each site in the lakes [51]. Total phosphorus (TP, $mg\ L^{-1}$) was determined in the laboratory using YSI 9500 photometer and YSI CR 3200 Thermoreactor (Xylem Analytics. Queensland, Australia) [52]. Quantifications added up to 648 data points.

2.3. Data Quality Control

Data for the sampling depth (SZ), sampling time (ST), and water temperature (WT) were analyzed at the three sites per lake to corroborate data reliability and the environmental conditions. As a first step, the WL and WT variance values were analyzed through non-parametric comparisons for each pair using the Wilcoxon test, at 5% statistical significance. Additionally, the WL, Chl-a, SD, WT, SZ, and ST values were transformed to natural logarithms as the original distributions of the variables were skewed, which resulted in linear relationships between variables. This was analyzed as SZ-Chl-a, SZ-SD, Chl-a-ST, and WT-ST, with a statistical dispersion of data analysis, followed by a parametric linear correlation (Pearson, $p < 0.05$) [53]. All analyses were carried out with the statistical program JMP® version 10 (SAS Institute, Inc., Cary, NC, USA).

The results obtained from the control data indicated that WL ($p > 0.0531$) and WT ($p > 0.3260$) were not statistically significant in the six lakes, since the greatest difference of the WL median among all samples was 0.24 m. Likewise, the WT values ($27.7 \pm 3.3\,°C$) were minimal for such tropical shallow lakes. The non-significant variation among the values of all samples of SZ-Chl-a ($r_{0.05\,(2),\,71} = 0.01244$, $p > 0.9173$) and SZ-SD ($r_{0.05\,(2),\,71} = 0.10082$, $p > 0.3994$) indicated that the data recorded for both parameters were non-statistically affected by the sampling of water collected at mid-depth in each sample throughout the hydrological year. The data dispersion between Chl-a-ST ($r_{0.05\,(2),\,71} = 0.1718$, $p > 0.1489$) and WT-ST ($r_{0.05\,(2),\,71} = 0.02988$, $p > 0.8032$) was also insignificant, which meant that the ST variation (8:00 a.m. to 01:00 p.m.) did not incur a bias in the Chl-a and SD data.

2.4. Data Analysis

Principal components analysis (PCA) was applied to the dataset of environmental variables (WL, SD, DOS, pH, EC, NH_4^+, NO_3^-, Chl-a, and TP) to identify temporal and spatial patterns linked to a strong indicator synthesis [54,55]. Except for pH, the remaining eight variables were used in the PCA with data normalized by logarithmic transformation (log x + 1) due to the presence of small numbers (for example, NH_4^+ and NO_3^-) and to eliminate their dependence on the units of measure used [53,56]. Based on these new values, the dissimilarities were calculated for the Euclidean distance, based on a correlation matrix [53,57].

The criteria used in those selected as meaningful principal components (PCs) corresponded to eigenvalues greater than 1 (Kaiser–Guttman criterion) and with a significant variation (Bartlett, $p < 0.05$) and the maximum percentage of variance explained [57]. Moreover, the variables with PC loadings greater than $|0.4|$ were selected [56] given the maximization of the data to contribute significantly to describe and represent the distribution patterns of the variables by each PC. This PCA was performed using the statistical software JMP® version 10 (SAS Institute, Inc., Cary, NC, USA).

The robust variables selected (water quality indicators) by the PCA were analyzed with descriptive statistics to help explain their expected overlapping distribution between TCL and IL or PCL. For this purpose, all values of the water quality indicators of TCL were used as the reference interval to estimate its overlap with IL and PCL. The reference interval of TCL (RI_{TCL}) was calculated through the mean and standard deviation ($\bar{x} \pm SD$) [34] of the data per each water quality indicator. The class size (CS) per each water quality indicator was only calculated for TCL using the formula: $CS_{TCL} = $ upper limit – lower limit, where the upper and lower limits are the range of the data of each water quality indicator [58]. The overlap interval is defined as the area where the data of the quality water indicators of IL and PCL coincide with the RI_{TCL} (see gray area or interval overlap in Figure 3). Finally, the overlap size (OS) for the three water quality indicators of PCL and IL was calculated using the formula: $OS_{IL\ or\ PCL} = $ upper limit $-$ lower limit, where the lower and upper limits are the upper limit datum and the lower limit datum of the overlap interval of IL or PCL [34]. Then, the overlapping between TCL and IL or PCL was expressed as the proportionality overlap (PO). PO was estimated per each one of the three water quality indicators using the formula: $PO = ((OS_{IL\ or\ PCL}) \times (CS_{TCL})^{-1})$, where $OS_{IL\ or\ PCL}$ and CS_{TCL} were already explained. For example, the reference interval of Chl-*a* in TCL (from 6.8 to 27.4 µg L^{-1}) allowed to calculate the $CS_{TCL} = 27.4 - 6.8 = 20.6$ µg L^{-1}. The overlap interval of PCL is between 7.7 and 22.6 µg L^{-1} since the data are placed within the RI_{TCL} (see gray area in Figure 3). If $OS_{PCL} = 22.6 - 7.7 = 14.9$ µg L^{-1} and $CS_{TCL} = 20.6$ µg L^{-1}, then the PO between PCL and TCL $= ((14.9$ µg L$^{-1}) \times (20.6$ µg L$^{-1})^{-1}) = 0.72$ (Table 1).

IL1=●, IL2=○, TCL3=◆, TCL4=◇, PCL5=■, PCL6=□
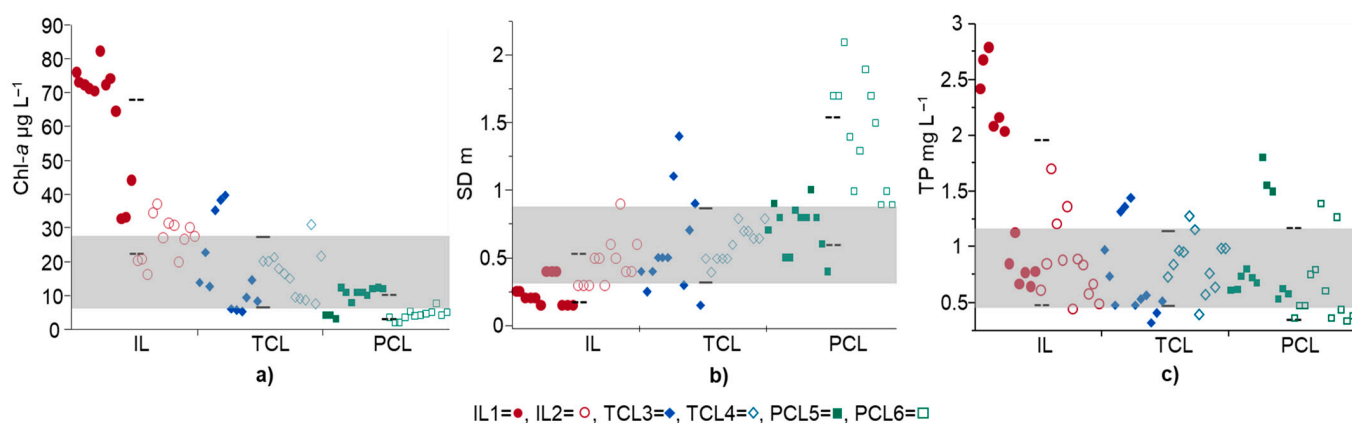
Figure 3. Distribution of the trophic indicator data, Chl-*a* (**a**), SD (**b**), and TP (**c**), for three conditions of surface hydraulic connection. IL = isolated lakes, TCL = temporally connected lakes, PCL = permanently connected lakes. Continuous black lines = TCL average and standard deviation ($\bar{x} \pm SD$). Dotted lines = IL and PCL average and standard deviation ($\bar{x} \pm SD$). Grey area = interval overlap of IL and PCL with TLC.

The data of the variables distributed in the CS_{TCL} and overlap interval of IL and PCL were employed to estimate the trophic state index (TSI) [47], and this was followed by the calculation of the deviations of TSI, TSI_{Chl-a}-TSI_{SD}, and TSI_{Chl-a}-TSI_{TP} to identify the limnological conditions [59] in the three hydraulic connection types of the six lakes.

Table 1. Proportionality overlap of indicator data distribution between TCL with IL and PCL and trophic state in three conditions of surface hydraulic connection. mean = $\bar{x}$; standard deviation = SD.

	Chl-*a*			SD			TP		
	µg L^{-1}			m			mg L^{-1}		
	IL	TCL	PCL	IL	TCL	PCL	IL	TCL	PCL
Recorded overlapping sites	7	17	10	14	19	13	14	16	14
Proportion of overlapping sites	0.41	-	0.59	0.74	-	0.68	0.88	-	0.88
Reference intervals ($\bar{x} \pm$ SD) (RI$_{TCL}$)	-	6.8–27.4	-	-	0.3–0.9	-	-	0.48–1.14	-
Class size of TLC (CS)		20.6			0.6			0.66	
Overlap intervals	16.2–27.3	-	7.7–22.6	0.3–0.6	-	0.3–0.9	0.49–1.12	-	0.48–0.8
Overlap size (OS)	11.1		14.9	0.3		0.6	0.63		0.32
Proportionality overlap (PO)	0.54	-	0.72	0.50	-	1.0	0.95	-	0.48
Trophic state	E	E	E	H	E	E	H	H	H

3. Results

3.1. Spatial and Temporal Fluctuation of Environmental Variables

A summary of the statistics of the nine environmental variables measured in six lakes is presented in Table S2. Variables related to the trophic state (Chl-*a*, SD, TP) varied in concentration from 2.3 to 82.3 µg L^{-1} for Chl-*a*, water transparency (measured with Secchi disk) ranged from 0.2 to 2.1 m, and TP ranged in concentration from 0.32 to 2.79 mg L^{-1}. The average SOD was 87% and the pH was 7.5. Average NO$_3^-$ and NH$_4^+$ concentrations were 4.30 and 0.62 mg L^{-1}, respectively. The average EC was 323 µS cm^{-1} and the WL was 1.0 m.

The first three PCs together explained 64.2% of the variance and seven variables (Ch-*a*, TP, SD, DOS, pH, NO$_3^-$, NH$_4^+$) had loadings greater than $|0.4|$ as a minimum in one PC (Table 2). The positive relationship between Chl-*a* and TP was observed in PC1 and these two showed a negative association with SD. These ratios separated the IL samples from the PCL samples, but both resulted in an overlapping distribution with the TCL samples. This PC explained 28% of the recorded total variance. This PC obtained eigenvalues greater than 1 ($p = 0.0001$). The three variables (Chl-*a*, SD, and TP) were considered strong indicators of water eutrophication for the three conditions of hydraulic connectivity in the six sampled lakes (Figure 4, Table 2).

Table 2. Loadings, eigenvalues, and PCA variance. Loadings greater than $|0.4|$ and eigenvalues greater than 1 in each PC are in bold. WL = water level, SD = Secchi disk depth, DOS = dissolved oxygen saturation, pH = hydrogen potential, EC = electrical conductivity, NH$_4^+$ = ammonium, NO$_3^-$ = nitrate, TP = total phosphorus, Chl-*a* = chlorophyll-*a*. $n = 648$.

Variables	PCI	PC2	PC3
WL	−0.136	0.120	−0.089
SD	**−0.478**	−0.055	0.313
DOS	−0.013	**0.677**	0.176
EC	−0.323	0.146	0.368
pH	0.190	**0.525**	0.343
TP	**0.493**	0.043	0.134
NH$_4^+$	0.164	−0.200	**0.590**
NO$_3^-$	0.193	**−0.424**	**0.481**
Chl-*a*	**0.553**	0.073	−0.113

Table 2. *Cont.*

Variables	PCI	PC2	PC3
Eigenvalue	2.521	1.834	1.428
Explained variance (%)	28.0	20.4	15.9
Accumulated variance (%)	28.0	48.4	64.2
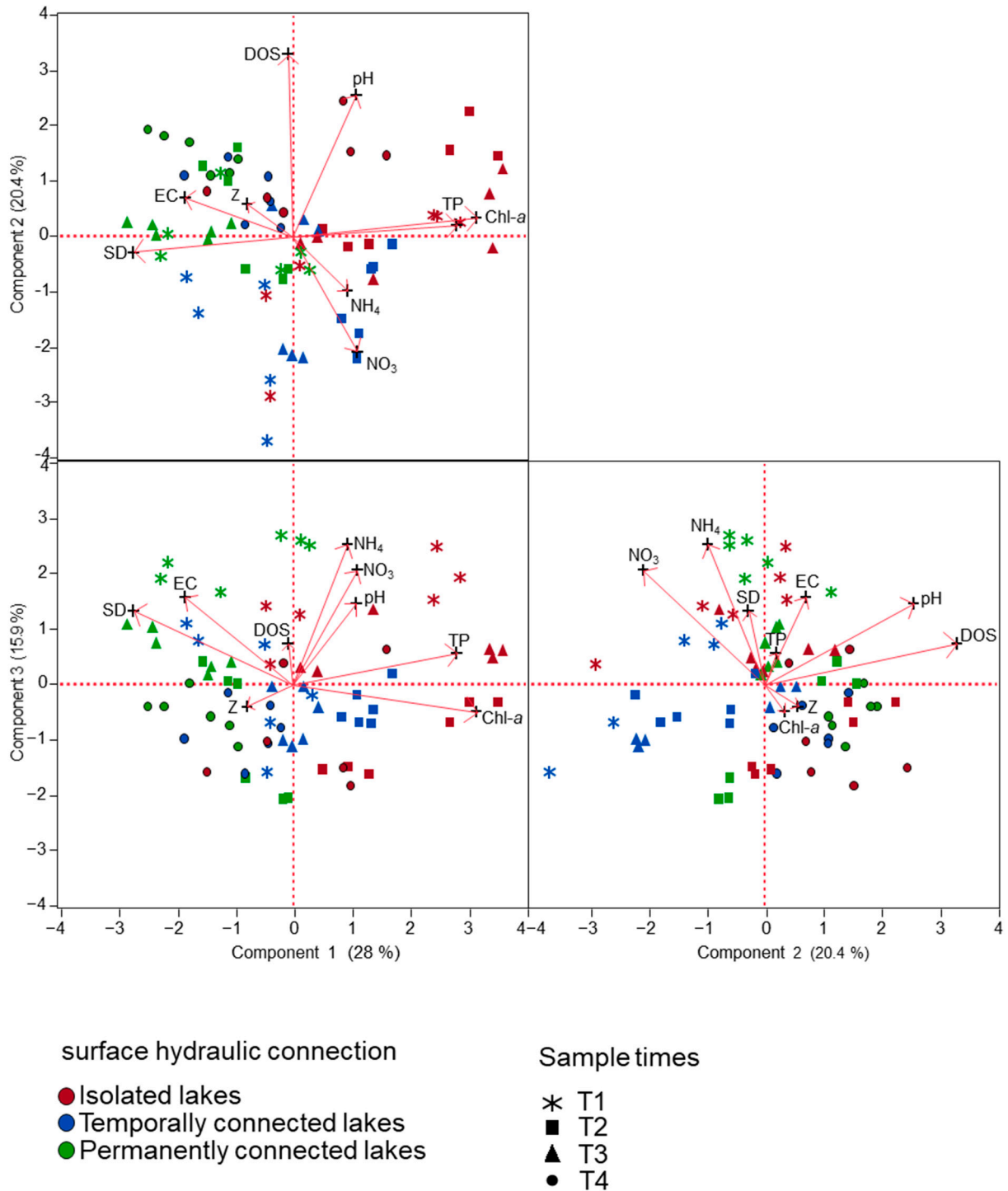
Figure 4. Biplot of the PCA (variables and scores) for water level (WL), Secchi disk (SD), dissolved oxygen saturation (DOS), hydrogen potential (pH), electrical conductivity (EC), ammonium (NH_4^+), nitrates (NO_3^-), total phosphorus (TP), and chlorophyll-*a* (Chl-*a*).

PC2 is used for demonstrating the positive relations among DOS, pH, and negative NO_3^-, and based on this the TCL and PCL are partially separated from the IL. PC2 accounted for 20.4% of the variance explained by the PCA (Figure 4, Table 2).

In PC3, loadings of NO_3^- and NH_4^+ were positively related and were not associated with connection conditions, but they were related to T1, and their explained variance was 15.9% (Table 2). Both PC2 and PC3 had eigenvalues greater than 1 ($p = 0.0001$) (Figure 4). The variables discarded in the PCA were EC and WL since both were not associated with significant changes in the limnetic condition (156–494 $\mu S\ cm^{-1}$) and with the expected inter-annual changes in depth, as it only varied from 0.3 to 2.3 m in the six lakes sampled (Table 2).

3.2. Overlapping of Water Quality Indicators under Three Surface Hydraulic Conditions

Overlap of the range of Chl-*a* concentrations in TCL (6.8 to 27.4 $\mu g\ L^{-1}$) resulted with the ranges of IL (16.2 to 27.3 $\mu g\ L^{-1}$) and PCL (7.7 and 22.6 $\mu g\ L^{-1}$) in 0.41 and 0.59 of the overlapping sites of IL and PCL, respectively (Table 1). The overlap of Chl-*a* at TCL sites had the lowest values in IL and the highest in PCL (Figure 3). In reference to the magnitude of variation of Chl-*a* values by hydraulic connection, the maximum variation (class size) was recorded in TCL, with 20.6 $\mu g\ L^{-1}$, followed by PCL and IL (Table 1). The proportionality overlap between the class size of TCL with IL was 0.54, and PCL had 0.72. These 3 class sizes included 34 overlapping values out of a total of 72 measured, and these represented 0.47 of the proportionality overlap between the 3 hydraulic connection conditions (Table 1). The 34 overlapping values are between 6.8 and 27.4 $\mu g\ L^{-1}$ of Chl-*a*. For ILs, the 17 Chl-*a* data greater than the upper range TCL value (27.4 $\mu g\ L^{-1}$) resulted between 29.9 and 82.3 $\mu g\ L^{-1}$. Among these, 12 records with the highest pigment concentrations (32.9–82.3 $\mu g\ L^{-1}$) were recorded in the lake 1 (IL1). Moreover, PCL had 14 records of Chl-*a* concentrations below the lower TCL range (6.8 $\mu g\ L^{-1}$), ranging from 2.3 to 5.7 $\mu g\ L^{-1}$, which in lake 6 (PCL6) showed the lowest Chl-*a* concentrations in 11 measurements (Figure 3).

In SD, there were complete overlaps between TCL and PCL (0.3 to 0.9 m), with ILs slightly decreased (0.3 to 0.6 m), which represented an overlap of sites of 0.68 and 0.74, respectively (Table 1). The overlap of TCL at the IL sites happened with most of their intermediate interval data, while the overlap of TCL with PCL yielded results with the lowest values of their interval (Figure 3). The proportionality overlap between the class size of TCL with PCL was total, and with IL was 0.5, which was linked to the maximum magnitude (0.6 m) of the class size in TCL and PCL (Table 1). From a total of 72 measured data points, 46 overlapping values were added in the 3 class sizes, which was equivalent to 0.64 proportionality overlap between IL, TCL, and PCL (Table 1). The 46 overlapping values were between 0.3 and 0.9 m for water transparency (SD). In opposition to Chl-*a*, in PCLs, the 11 SD values greater than the upper TCL interval value (0.9 m) ranged from 1 to 2.1 m and 10 records in PCL6 stood out for higher light passage. In contrast, 9 IL measurements of the SD records were lower than the lower TCL interval value (0.3 m), which ranged from 0.15 to 0.25 m only in IL1 (Figure 3).

Although the range of TP in PCL (0.48 to 0.80 mg L^{-1}) was narrower than those of TCL (0.48 to 1.14 mg L^{-1}) and IL (0.49 to 1.12 mg L^{-1}), the overlap of the range of TCL with IL and PCL was 0.88 (Figure 3, Table 1). Between TCL and PCL, the proportionality overlap between the class size was 0.48, and IL was 0.95 (Table 1). In the 3 class sizes, 44 overlapping values were recorded out of 72 measurements, which corresponded to a 0.69 proportionality overlap for the 3 surface hydraulic connection conditions (Table 1). The 44 overlapping values were between 0.48 and 1.14 mg L^{-1} of TP. Similar to Chl-*a*, 9 TP concentrations in IL were greater than the upper range value of TCL (1.14 $\mu g\ L^{-1}$), with a fluctuation from 1.20 to 2.79 $\mu g\ L^{-1}$. Six of these values in IL1 were the nutrient's maximum values, while five of the twelve records measured in PCL6 resulted with the lowest TP concentrations (0.34 to 0.44 $\mu g\ L^{-1}$) and lower than the lower range value of TCL (0.48 $\mu g\ L^{-1}$) (Figure 3). Between TCL and PCL, the overlap between SD (1.0) and

Chl-*a* (0.72) was outstanding. Whereas, between TCL and IL, the PT overlapped in 0.95, and mostly with IL2 and PCL5 values.

3.3. Trophic State under Different Surface Hydraulic Conditions

Based on the Chl-*a* concentrations, the three types of surface hydraulic connections were eutrophic; likewise, with the SD data, the TCL and PCL were eutrophic, and in the ILs they stood out for their hypereutrophic condition. Similarly, due to the PT concentrations, the hypereutrophic state stood out in the three SHC conditions (Table 1). Deviations of TSI_{Chl-a} from those of TSI_{SD} and TSI_{TP} resulted in negative relationships between TSI_{Chl-a} and TSI_{SD}, as well as between TSI_{Chl-a} and TSI_{TP}, for both TLC, PCL, and IL.

4. Discussion

4.1. Water Quality Indicators in Lakes with Different Surface Hydraulic Conditions

The three indicators (Chl-*a*, SD, and TP) that explained the greatest variability in PC1 in this study coincided with those used to estimate the trophic state [48], since the changes in phytoplankton biomass, SD, and TP in floodplain lakes were associated with different conditions of SHC, under scarce variation in water levels [29,60]. Furthermore, these three indicators are relevant in tropical and subtropical floodplain systems since phytoplankton biomass is an important source of carbon for aquatic organisms [49].

The expected inverse relationship between Chl-*a* and SD has been explained by the fact that phytoplankton biomass depends on light intensity [61]. In the study area, this inverse relationship was straightened by the TP surplus effect. However, the fluctuations in light intensity are multi-scale and multifactorial, being linked to the combined effects of the daily and seasonal variations, the latitudinal location, the quantity and quality of suspended solids, and dissolved organic substances [59,62]. Moreover, the light refraction is frequently limited by re-suspension of materials in continuously warm polymictic shallow lakes [63,64]. Then, its effect on phytoplankton biomass was not noticeable because the maximum water turbidity was under 90 NTU in the six lakes sampled in this study.

The direct relationship between Chl-*a* and TP can be linked to the conversion of inorganic nutrients to organic nutrients in sediments, which is typically attributed to algal and vegetative communities in floodplains [65]. However, the internal TP enrichment is generated through autochthonous organic matter and the exchange with the sediment in conditions of reduced intra-annual fluctuations in water levels [13,29]. Furthermore, the phosphorus enrichment generated by allochthonous matter provided by runoff can be attributed to persistent inputs of urban and agricultural wastewater [16,24,27,28,46,61,66]. In addition, increased TP from sediment resuspension and nutrient assimilation changes the composition of the phytoplankton community, and favors cyanobacterial blooms, which can cause light limitation conditions, as analyzed in a shallow lake in the central part of Jutland, Denmark [67].

The variables DOS, pH, NO_3^-, and NH_4^+ were partially linked to any of the three SHC conditions or to intra-annual variation, and therefore were discarded as indicators. In this regard, ILs stood out in terms of maximum values of DO ($95\% \pm 55\%$) and pH (7.8 ± 0.8) considering the excess algal biomass in urbanized ILs within the MAV as well as in other regions [27,68]. In TCLs, NO_3^- data (<1 mg L^{-1}) were attributed to its assimilation by submerged aquatic macrophytes in preserved lakes [69]. While most of the NO_3^- and NH_4^+ values were greater than 1 mg L^{-1} in all data recorded for the IL, 50% in the PCL at T1, this is similar in lakes of the Usumacinta River and Taihu Lake basins [9,70].

Regarding the two variables discarded in the PCA, the WL amplitude was narrow (Table S2) relative to that recorded (1.5 to 4.9 m) in the basin floodplain [47]. This reduction in WL has been linked to the limited or non-existent hydraulic interconnection between lakes and rivers on the plains of the MAV, as a result of the operation and construction of hydraulic and urban infrastructure [18,36,42]. The second variable (EC) was included in the PCA because of its significant relationship with Chl-*a* [49], but it lacked statisti-

cal correlations with the other eight variables and only reiterated the limnetic condition (Table S2) [71] in the sampled lakes.

4.2. Overlapping of Water Quality Indicators in Three Surface Hydraulic Conditions

In the study area, TLCs showed the greatest variation in the concentrations of the three indicators, Chl-*a*, SD, and TP (Table 1), which was reflected in their proportionality overlap with PCL and IL. This amplitude in the variation of indicators in TCL has been related to seasonal flooding water that induces changes in the physicochemistry of water in temporary lakes in the Grijalva basin, the Amazon River, and the Poyang Lake floodplain [11,12,28]. However, the restricted temporal effect of flooding in the study area by the embankments reduced the expected seasonal variation of the water levels. Thus, the effect of the embankments helps to support that the higher variation detected in the concentrations of the three indicators is mainly explained by the limited SHC, which in turn is linked to a higher water residence rate [7]. In the case of Chl-*a*, the proportionality overlap of TCL was slightly greater with PCL than with IL. In this regard, overlapping Chl-*a* concentrations were also recorded between permanently connected lakes and temporary lakes in Poyang Lake's floodplain wetlands, altered in their SHC [12].

All Chl-*a* values that overlapped between 6.8 and 27.4 μg L^{-1} in the three conditions of SHC were eutrophic [15,48]. This result is consistent with the eutrophic conditions recorded in lakes isolated by artificial embankments and receiving urban inputs, as well as in TCLs regulated in their water level and in permanently connected lakes affected by urban wastewater [12,16,30,72,73].

The total overlap in SD stood out between the TLC and PCL, although 84% and 92% of the data were eutrophic ($\geq$0.5 m), respectively, and the SD variation was minimal in the three SHCs. Based on the above, the magnitude and amplitude of water transparency is high in TCL during the annual cycle in wetlands that are connected to free-flowing rivers [30]. However, in floodplains with dammed rivers, seasonal shallow lakes show intra-annual fluctuations opposite to the Secchi disk depth, which was mainly attributed to surface runoff and continuous sediment discharge causing permanent turbidity in seasonal lakes [16,74]. In this context, the eutrophic state of shallow lakes temporarily and permanently connected to their upstream dammed rivers was explained using SD values [16,75]. In contrast, the ILs stood out for the decrease in the variation of SD values, since most of the records (64%) were hypereutrophic (<0.5 m) [15,76]. In hypereutrophic tropical ILs, the restriction in the passage of light is frequent and its variation is minimal due to the re-suspension of materials [27,77].

Finally, the overlap of the variation of TP concentrations in TCLs and ILs was greater compared to the concentrations of PCLs. However, all three conditions of SHC were hypereutrophic according to [15], as the superimposed TP concentrations equaled or exceeded 0.480 mg L^{-1}. Thus, the nutrient enrichment in the studied lakes with limited or non-existent interconnections was independent of the conditions of SHC. In this context, the hypereutrophication condition has been recorded in other tropical lakes altered by hydraulic infrastructure, resulting in a loss of lateral flooding, restricted water level variation, and an increased water residence time, which affect the dynamics of bioavailable organic phosphorus [28,29,78,79]. The increase of TP concentrations and hypereutrophication in the sampled lakes may be related to autochthonous and allochthonous organic matter, sediment resuspension, and runoff of wastewater from the MAV and from agricultural areas in the rural zone, which was recorded in this and other study areas [8,27,46,68,80,81].

Regarding the non-overlapping values of Chl-*a*, TP, and SD between IL and PCL with TCL, the variation of the first two was expected to be inverse to SD due to TP assimilation by phytoplankton that influences the passage of light [13,61]. Accordingly, the records measured in IL1 and PCL6 stood out at the extremes of the upper overlap for Chl-*a* and TP, and lower for SD (Figure 3). In the case of Chl-*a* and TP, of their 27 non-overlapping values outside the class size, 15 were IL1 and 12 were IL2. Moreover, from the 11 non-

overlapping SD data outside the class size, 1 and 10 values were recorded in PCL5 and PCL6, respectively (Figure 3).

The maximum Chl-*a* and TP concentrations in IL, located above the upper TCL range, are tied to the hydraulic and urban disturbance recorded in the six lakes included in this study, since IL1 has been reported as eutrophicated with elevated TP, Chl-*a*, and inorganic nitrogen values since the 1990s [82] and currently has low fish diversity related to its hydraulic isolation condition [42]. Similarly, hydraulically isolated lakes registered eutrophic or hypereutrophic conditions in the Grijalva, Illinois, and Atchafalaya River basins [6,14,27]. The biggest overlap of TCL with IL2 is attributed to the fact that this lake has a degree of urban disturbance lower than IL1, because it is at the outer limit of the urban sprawl [37,83].

The higher percentage of maximum SD values in PCL6 is linked to its less disturbed condition with respect to PCL5. The most notable difference between the two lakes is associated with the presence of submerged rooted macrophytes in PLC6, as these macrophytes have been frequently tied to higher transparency and lower Chl-*a* concentration in lakes [14,69], which is also reflected in the conservation of environmental functions and services, such as water quality, trophic status, and species richness [67,84,85].

4.3. Variation of Trophic State Linked to Surface Hydraulic Conditions

The predominant eutrophication in the six shallow lakes sampled in the three SHCs was caused by the TP surplus, according to the interpretation of the trophic state index deviations [58]. These persistent high TP concentrations are associated with the combination of organic matter accumulation and the modifications to natural flood cycles by infrastructure in the upstream floodplain, as has been reported in other watersheds [21,86–88]. In the case of the TCL and PCL of the study area, runoff comes from agricultural and livestock activities [28,81], with similar impacts in other aquatic ecosystems [69,70], while in ILs, TP concentrations are further exacerbated by the addition of runoff from urban waste activities and infrastructure [27,28,72]. Surplus TP related to urbanization, agriculture, and hydraulic infrastructure has been reported in other lakes located in different basins [8,60,78,89]. Persistent hypereutrophication by TP negatively affects lake functions by excessively increasing algal biomass, and in turn causes the decline of rooted submerged macrophytes and decreases aquatic fauna diversity [42,88,90].

5. Conclusions

The hypothesis of this study was partially proven because the values of the three water quality indicators (Chl-*a*, SD, TP) in TCL registered an overlap greater than 0.72 in relation to PCL and IL. In the study area, the surplus of TP measured in all lakes, particularly in the ILs, indicates the effect of the degree of disturbance cause by urbanization. However, the PT surplus was attenuated in a rural lake (PCL6) by the presence of submerged rooted macrophytes. Considering the high overlap of the three water quality indicators between TCL, PCL, and IL, it is necessary to verify whether these results can be applied as a predictive and preventive tool for conservation management, through an analysis on a more representative spatial and temporal scale of the variations measured in lakes located in tropical coastal plains.

References

1. Amoros, C.; Bornette, G. Connectivity and biocomplexity in waterbodies of riverine floodplains. *Freshw. Biol.* **2002**, *47*, 761–776. [CrossRef]
2. Gurnell, A.M.; Rinaldi, M.; Belletti, B.; Bizzi, S.; Blamauer, B.; Braca, G.; Buijse, A.D.; Bussettini, M.; Camenen, B.; Comiti, F.; et al. A multiscale hierarchical framework for developing understanding of river behaviour to support river management. *Aquat. Sci.* **2016**, *78*, 1–16. [CrossRef]
3. Shen, M.; Liu, X. Assessing the effects of lateral hydrological connectivity alteration on freshwater ecosystems: A meta-analysis. *Ecol. Indic.* **2021**, *125*, 107572. [CrossRef]
4. Junk, W.J.; Bayley, P.B.; Sparks, R.E. The flood pulse concept in river-floodplain systems. In Proceedings of the International Large River Symposium, Honey Harbour, ON, Canada, 14 September 1986; Dodge, D.P., Ed.; Canadian Special Publication of Fisheries and Aquatic Sciences: Ontario, Canada, 1989; pp. 110–127.
5. Racchetti, E.; Bartoli, M.; Soana, E.; Longhi, D.; Christian, R.R.; Pinardi, M.; Viaroli, P. Influence of hydrological connectivity of riverine wetlands on nitrogen removal via denitrification. *Biogeochemistry* **2011**, *103*, 335–354. [CrossRef]
6. Jones, C.N.; Scott, D.T.; Edwards, B.L.; Keim, R.F. Perirheic mixing and biogeochemical processing in flow-through and backwater floodplain wetlands. *Water Resour. Res.* **2014**, *50*, 7394–7405. [CrossRef]
7. Fritz, K.M.; Schofield, K.A.; Alexander, L.C.; McManus, M.G.; Golden, H.E.; Lane, C.R.; Kepner, W.G.; Le Duc, S.D.; DeMeester, J.E.; Pollard, A.I. Physical and chemical connectivity of streams and riparian wetlands to downstream waters: A synthesis. *J. Am. Water Resour. As.* **2018**, *54*, 323–345. [CrossRef]
8. de Wilde, M.D.; Puijalon, S.; Vallier, F.; Bornette, G. Physico-chemical consequences of water-level decreases in wetlands. *Wetlands* **2015**, *35*, 683–694. [CrossRef]
9. Cruz-Ramírez, A.K.; Salcedo, M.A.; Sánchez, A.J.; Barba Macías, E.; Mendoza Palacios, J.D. Relationship among physicochemical conditions, chlorophyll-*a* concentration, and water level in a tropical river–floodplain system. *Int. J. Environ. Sci. Technol.* **2019**, *16*, 3869–3876. [CrossRef]
10. Larsen, L.G.; Harvey, J.W.; Maglio, M. Mechanisms of nutrient retention and its relation to flow connectivity in river–floodplain corridors. *Freshw. Biol.* **2015**, *34*, 187–205. [CrossRef]
11. Park, E.; Latrubesse, E.M. The hydro-geomorphologic complexity of the lower Amazon River floodplain and hydrological connectivity assessed by remote sensing and field control. *Remote Sens. Environ.* **2017**, *198*, 321–332. [CrossRef]
12. Li, Y.; Zhang, Q.; Cai, Y.; Tan, Z.; Wu, H.; Liu, X.; Yao, J. Hydrodynamic investigation of surface hydrological connectivity and its effects on the water quality of seasonal lakes: Insights from a complex floodplain setting (Poyang Lake, China). *Sci. Total Environ.* **2019**, *660*, 245–259. [CrossRef] [PubMed]
13. Jones, C.N.; Scott, D.T.; Guth, C.R.; Hester, E.T.; Hession, W.C. Seasonal variation in floodplain biogeochemical processing in a restored headwater stream. *Environ. Sci. Technol.* **2015**, *49*, 13190–13198. [CrossRef] [PubMed]
14. Sparks, R.E.; Blodgett, K.D.; Casper, A.F.; Hagy, H.M.; Lemke, M.J.; Velho, L.F.M.; Rodrigues, L.C. Why experiment with success? Opportunities and risks in applying assessment and adaptive management to the Emiquon floodplain restoration project. *Hydrobiologia* **2017**, *804*, 177–200. [CrossRef]

15. Carlson, R.E.; Simpson, J. *A Coordinator's Guide to Volunteer Lake Monitoring Methods*; North American Lake Management Society: Colorado Springs, CO, USA, 1996; p. 96.

16. Jeppesen, E.; Brucet, S.; Naselli-Flores, L.; Papastergiadou, E.; Stefanidis, K.; Nõges, T.; Nõges, P.; Attayde, J.L.; Zohary, T.; Coppens, J.; et al. Ecological impacts of global warming and water abstraction on lakes and reservoirs due to changes in water level and related changes in salinity. *Hydrobiologia* **2015**, *750*, 201–227. [CrossRef]

17. Thorp, J.H.; Thoms, M.C.; Delong, M.D. The riverine ecosystem synthesis: Biocomplexity in river networks across space and time. *River Res. Appl.* **2006**, *22*, 123–147. [CrossRef]

18. Sánchez, A.J.; Salcedo, M.A.; Florido, R.; Mendoza, J.D.; Ruiz-Carrera, V.; Álvarez-Pliego, N. Ciclos de inundación y conservación de servicios ambientales en la cuenca baja de los ríos Grijalva-Usumacinta. *ContactoS* **2015**, *97*, 5–14.

19. Zhang, Q.; Dong, X.; Chen, Y.; Yang, X.; Xu, M.; Davidson, T.A.; Jeppesen, E. Hydrological alterations as the major driver on environmental change in a floodplain Lake Poyang (China): Evidence from monitoring and sediment records. *J. Great Lakes Res.* **2018**, *44*, 377–387. [CrossRef]

20. Poff, N.L.; Olden, J.D.; Merritt, D.M.; Pepin, D.M. Homogenization of regional river dynamics by dams and global biodiversity implications. *Proc. Natl. Acad. Sci. USA* **2007**, *104*, 5732–5737. [CrossRef]

21. Poff, N.L.; Schmidt, J.C. How dams can go with the flow, small changes to water flow regimes from dams can help to restore river ecosystems. *Science* **2016**, *353*, 1099–1100. [CrossRef]

22. Wolter, C.; Buijse, A.D.; Parasiewicz, P. Temporal and spatial patterns of fish response to hydromorphological processes. *River Res. Appl.* **2016**, *32*, 190–201. [CrossRef]

23. Leira, M.; Cantonati, M. Effects of water-level fluctuations on lakes: An annotated bibliography. *Hydrobiologia* **2008**, *613*, 171–184. [CrossRef]

24. Obolewski, K.; Glińska-Lewczuk, K.; Bąkowska, M. From isolation to connectivity: The effect of floodplain lake restoration on sediments as habitats for macroinvertebrate communities. *Aquat. Sci.* **2018**, *80*, 4. [CrossRef]

25. Bunn, S.; Arthington, A.H. Basic principles and ecological consequences of altered flow regimes for aquatic biodiversity. *Environ. Manag.* **2002**, *30*, 492–500. [CrossRef] [PubMed]

26. Dai, X.; Yang, G.; Wang, R.; Li, Y. The effect of the Changjiang River on water regimes of its tributary Lake East Dongting. *J. Geogr. Sci.* **2018**, *28*, 1072–1084. [CrossRef]

27. Sánchez, A.J.; Salcedo, M.A.; Macossay-Córtez, A.A.; Feria-Díaz, Y.; Vázquez, L.; Ovando, N.; Rosado, L. Calidad ambiental de la laguna urbana La Pólvora en la cuenca del Río Grijalva. *Tecnol. Cienc. Agua* **2012**, *3*, 143–152.

28. Cruz-Ramírez, A.K.; Salcedo, M.A.; Sánchez, A.J.; Mendoza Palacios, J.D.; Barba Macías, E.; Álvarez-Pliego, N.; Florido, R. Intra-annual variation of chlorophyll-*a* and nutrients in a hydraulically perturbed river-floodplain system in the Grijalva River basin. *Hidrobiológica* **2019**, *29*, 163–170. [CrossRef]

29. Reckendorfer, W.; Funk, A.; Gschöpf, C.; Hein, T.; Schiemer, F. Aquatic ecosystem functions of an isolated floodplain and their implications for flood retention and management. *J. Appl. Ecol.* **2013**, *50*, 119–128. [CrossRef]

30. Affonso, A.G.; Quieroz, H.L.; Novo, E.M.L.N. Abiotic variability among different aquatic systems of the central Amazon floodplain during drought and flood events. *Braz. J.* **2015**, *75*, 60–69. [CrossRef]

31. Walalite, T.; Dekker, S.C.; Keizer, F.M.; Kardel, I.; Schot, P.P.; DeJong, S.M.; Wassen, M.J. Flood Water Hydrochemistry Patterns Suggest Floodplain Sink Function for Dissolved Solids from the Songkhram Monsoon River (Thailand). *Wetlands* **2016**, *36*, 995–1008. [CrossRef]

32. Science for Environment Policy. *Identifying Emerging Risks for Environmental Policies*; Future Brief 13; Brief Produced for the European Commission DG Environment by the Science Communication Unit, UWE Bristol: Bristol, UK, 2016.

33. Hidalgo, E.A.; Gómez, A.O.; Arreola, M.M. Manatees Mortality Analysis at Los Bitzales, Tabasco by Remote Sensing. *Int. J. Latest Res. Eng. Technol.* **2019**, *5*, 1–15.

34. Ramos-Guajardo, A.B.; González-Rodríguez, G.; Colubi, A. Testing the degree of overlap for the expected value of random intervals. *Int. J. Approx. Reason.* **2020**, *119*, 1–19. [CrossRef]

35. Zavala-Cruz, J.; Jiménez-Ramírez, R.; Palma-López, D.; Bautista-Zúñiga, F.; Gavi-Reyes, F. Paisajes geomorfológicos: Base para el levantamiento de suelos en Tabasco, México. *Ecosist. Recur. Agropec.* **2016**, *3*, 163–164. [CrossRef]

36. Arreguín-Cortés, F.; Rubio-Gutiérrez, H.; Domínguez-Mora, R.; de Luna-Cruz, F. Análisis de las inundaciones en la planicie tabasqueña en el periodo 1995–2010. *Tecnol. Cienc. Agua* **2014**, *5*, 5–32.

37. Palomeque de la Cruz, M.A.; Galindo, A.; Sánchez, A.J.; Escalona, M.J. Pérdida de humedales y vegetación por urbanización en la cuenca del Río Grijalva, México. *Investig. Geogr.* **2017**, *68*, 151–172. [CrossRef]

38. Navarro, J.M.; Toledo, H. Transformación de la cuenca del Río Grijalva. Revista Noticias. *Asoc. Mex. De Ing. Portuaria* **2004**, *4*, 11–22.

39. Comisión Nacional del Agua (CONAGUA). Atlas del Agua en México. 2018. Available online: http://sina.conagua.gob.mx/publicaciones/AAM_2018.pdf (accessed on 24 June 2018).

40. Alcérreca-Huerta, J.C.; Callejas-Jiménez, M.E.; Carrillo, L.; Castillo, M.M. Dam implications on salt-water intrusion and land use within a tropical estuarine environment of the Gulf of Mexico. *Sci. Total Environ.* **2019**, *652*, 1102–1112. [CrossRef] [PubMed]

41. Mendoza, A.; Soto-Cortés, G.; Priego-Hernández, G.; Rivera-Trejo, F. Historical description of the morphology and hydraulic behavior of a bifurcation in the lowlands of the Grijalva River Basin, Mexico. *Catena* **2019**, *176*, 343–351. [CrossRef]

42. Sánchez, A.J.; Álvarez-Pliego, N.; Espinosa-Pérez, H.; Florido, R.; Macossay-Cortez, A.; Barba, E.; Salcedo, M.A.; Garrido-Mora, A. Species richness of urban and rural fish assemblages in the Grijalva Basin floodplain, southern Gulf of Mexico. *Cybium* **2019**, *43*, 239–254. [CrossRef]

43. Instituto de Planeación y Desarrollo Urbano (IMPLAN). Programa de Desarrollo Urbano del Centro de Población de la Ciudad de Villahermosa y Centros Metropolitanos del Municipio de Centro, Tabasco 2008–2030. 2008. Available online: https://tabasco.gob.mx/programas-de-desarrollo-urbano-municipios. (accessed on 15 April 2016).

44. Instituto Nacional de Estadística y Geografía (INEGI). Delimitación de las Zonas Metropolitanas de México 2015. 2018. Available online: https://www.gob.mx/conapo/documentos/delimitacion-de-las-zonas-metropolitanas-de-mexico-2015. (accessed on 12 May 2019).

45. Instituto Nacional de Estadística y Geografía (INEGI). Simulador de Flujos de Agua de Cuencas Hidrográficas Versión 4.0. 2021. Available online: https://antares.inegi.org.mx/analisis/red_hidro/siatl/. (accessed on 12 April 2021).

46. Salcedo, M.A.; Sánchez, A.J.; Cruz-Ramírez, A.K.; Álvarez-Pliego, N.; Florido, R.; Ruiz-Carrera, V.; Garrido, A.; Alejo-Díaz, R. Aplicación del índice de calidad del agua (WQI-NSF) en lagunas metropolitanas y rurales. *Agroproductividad* **2018**, *11*, 81–86.

47. Comisión Nacional del Agua (CONAGUA). Banco Nacional de Datos de Aguas Superficiales. 2016. Available online: http://app.conagua.gob.mx/bandas/ (accessed on 12 May 2016).

48. Carlson, R.E. A trophic state index for lakes. *Limnol. Oceanogr.* **1977**, *22*, 361–369. [CrossRef]

49. Rocha, R.R.A.; Thomaz, S.M.; Carvalho, P.; Gomes, L.C. Modeling chlorophyll-*a* and dissolved oxygen concentration in tropical floodplain lakes (Paraná River, Brazil). *Braz. J. Biol.* **2009**, *69*, 491–500. [CrossRef] [PubMed]

50. Zhang, Y.; Yang, G.; Li, B.; Cai, Y.; Chen, Y. Using eutrophication and ecological indicators to assess ecosystem condition in Poyang Lake, a Yangtze-connected lake. *Aquat. Ecosyst. Health* **2016**, *19*, 29–39. [CrossRef]

51. Uzarski, D.G.; Wilcox, D.A.; Brady, V.J.; Cooper, M.J.; Albert, D.A.; Ciborowski, J.J.H.; Danz, N.P.; Garwood, A.; Gathman, J.P.; Thomas, M.G.; et al. Leveraging a Landscape-Level Monitoring and Assessment Program for Developing Resilient Shorelines throughout the Laurentian Great Lakes. *Wetlands* **2019**, *39*, 1357–1366. [CrossRef]

52. American Public Health Association (APHA). *Standard Methods for the Examination of Water and Wastewater*; American Public Health Association, American Water Works Association, Water Environment Federation: Washington, DC, USA, 1998.

53. Zar, J.H. *Biostatistical Analysis*, 5th ed.; Prentice Hall: Englewood Cliffs, NJ, USA, 2010; ISBN 978-0-13-100846-5.

54. Diamantini, E.; Lutz, S.R.; Mallucci, S.; Majone, B.; Merz, R.; Bellin, A. Driver detection of water quality trends in three large European river basins. *Sci. Total Environ.* **2018**, *612*, 49–62. [CrossRef]

55. Yang, K.; Yu, Z.; Luo, Y.; Yang, Y.; Zhao, L.; Zhou, X. Spatial and temporal variations in the relationship between lake water surface temperatures and water quality—A case study of Dianchi Lake. *Sci. Total Environ.* **2018**, *624*, 859–871. [CrossRef]

56. Weilhoefer, C.L.; Yangdong, P.; Eppard, S. The effects of river floodwaters on floodplain wetland water quality and diatom assemblages. *Wetlands* **2008**, *28*, 473–486. [CrossRef]

57. Legendre, P.; Legendre, L. *Numerical Ecology*, 2nd ed.; Elsevier: Amsterdam, The Netherlands, 2003; ISBN 0-444-89250-8.

58. Mohammed, M.B.; Adam, M.B.; Zulkafli, H.S.; Ali, N. Improved Frequency Table with Application to Environmental Data. *Math. Stat.* **2020**, *8*, 201–210. [CrossRef]

59. Carlson, R.E.; Havens, K.E. Simple graphical methods for the interpretation of relationships between trophic state variables. *Lake Reserv. Manag.* **2005**, *21*, 107–118. [CrossRef]

60. Yuan, Y.; Jiang, M.; Liu, X.; Yu, H.; Otte, M.L.; Ma, C.; Her, Y.G. Environmental variables influencing phytoplankton communities in hydrologically connected aquatic habitats in the Lake Xingkai basin. *Ecol. Indic.* **2018**, *91*, 1–12. [CrossRef]

61. Liu, X.; Qian, K.; Chen, Y.; Gao, J.A. comparison of factors influencing the summer phytoplankton biomass in China's three largest freshwater lakes: Poyang, Dongting, and Taihu. *Hydrobiologia* **2017**, *792*, 283–302. [CrossRef]

62. Wetzel, R.G. *Limnology Lake and River Ecosystems*, 3rd ed.; Academic Press: San Diego, CA, USA, 2001; ISBN 10: 0-12-744760-1.

63. Scheffer, M. *Ecology of Shallow Lakes*; Chapman and Hall: London, UK, 1998; ISBN 9780412749209.

64. Blottière, L.; Jaffar-Bandjee, M.; Jacquet, S.; Millot, A.; Hulot, F.D. Effect of mixing on the pelagic food web in shallow lakes. *Freshw. Biol.* **2017**, *62*, 161–177. [CrossRef]

65. Vymazal, J. Removal of nutrients in various types of constructed wetlands. *Sci. Total Environ.* **2007**, *380*, 48–65. [CrossRef] [PubMed]

66. Pinilla, G. An index of limnological conditions for urban wetlands of Bogota city, Colombia. *Ecol. Indic.* **2010**, *10*, 848–856. [CrossRef]

67. Andersen, T.K.; Nielsen, A.; Jeppesen, E.; Hu, F.; Bolding, K.; Liu, Z.; Søndergaard, M.L.S.; Johansson, L.S.; Trolle, D. Predicting ecosystem state changes in shallow lakes using an aquatic ecosystem model: Lake Hinge, Denmark, an example. *Ecol. Appl.* **2020**, *30*, e02160. [CrossRef] [PubMed]

68. Balan, A.; Obolewski, A.; Luca, M.; Cretescu, U. Use of macroinvertebrates for assessment of restoration works influence on the habitat in floodplain lakes. *Environ. Eng. Manag. J.* **2017**, *16*, 969–978. [CrossRef]

69. Szpakowska, B.; Świerk, D.; Pajchrowska, M.; Gołdyn, R. Verifying the usefulness of macrophytes as an indicator of the status of small waterbodies. *Sci. Total Environ.* **2021**, *798*, 149279. [CrossRef]

70. Zhu, Q.D.; Sun, J.H.; Hua, G.F.; Wang, J.H.; Wang, H. Runoff characteristics and non-point source pollution analysis in the Taihu Lake Basin: A case study of the town of Xueyan, China. *Environ. Sci. Pollut. Res.* **2015**, *22*, 15029–15036. [CrossRef]

71. Cowardin, L.M.; Carter, V.; Golet, F.C.; LaRoe, E.T. *Classification of Wetlands and Deepwater Habitats of the United States*; US Department of the Interior, US, Fish and Wildlife Service: Washington, DC, USA, 1979.

72. Xu, F.L.; Jiao, Y. Trophic classification for lakes. In *Encyclopedia of Ecology*, 2nd ed.; Fath, B., Ed.; Elsevier: Amsterdam, The Netherlands, 2019; ISBN 9780444641304.

73. Zou, W.; Zhu, G.; Cai, Y.; Vilmi, A.; Xu, H.; Zhu, M.; Gong, Z.; Zhang, Y.; Qin, B. Relationships between nutrient, chlorophyll *a* and Secchi depth in lakes of the Chinese Eastern Plains ecoregion: Implications for eutrophication management. *J. Environ. Manag.* **2020**, *260*, 1–9. [CrossRef]

74. Ren, J.; Zheng, Z.; Li, Y.; Lv, G.; Wuang, Q.; Lyu, H.; Huang, C.; Liu, G.; Du, C.; Mu, M.; et al. Remote observation of water clarity patterns in Three Gorges Reservoir and Dongting Lake of China and their probable linkage to the Three Gorges Dam based on Landsat 8 imagery. *Sci. Total Environ.* **2018**, *625*, 1554–1566. [CrossRef]

75. Carhart, A.M.; Kalas, J.E.; Rogala, J.T.; Rohweder, J.J.; Drake, D.C.; Houser, J.N. Understanding constraints on submersed vegetation distribution in a large, floodplain river: The role of water level fluctuations, water clarity and river geomorphology. *Wetlands* **2021**, *41*, 1–15. [CrossRef]

76. Sheela, A.M.; Letha, J.; Joseph, S. Environmental status of a tropical lake system. *Environ. Monit. Assess.* **2011**, *180*, 427–449. [CrossRef] [PubMed]

77. de Amo, V.E.; Ernandes-Silva, J.; Moi, D.A.; Mormul, R.P. Hydrological connectivity drives the propagule pressure of *Limnoperna fortunei* (Dunker, 1857) in a tropical river–floodplain system. *Hydrobiologia* **2021**, *848*, 2043–2053. [CrossRef]

78. Wu, P.; Qin, B.; Yu, G. Estimates of long-term water total phosphorus (TP) concentrations in three large shallow lakes in the Yangtze River basin, China. *Environ. Sci. Pollut. Res.* **2016**, *23*, 4938–4948. [CrossRef] [PubMed]

79. Wang, Y.; Molinos, J.G.; Shi, L.; Zhang, M.; Wu, Z.; Zhang, H.; Xu, J. Drivers and Changes of the Poyang Lake Wetland Ecosystem. *Wetlands* **2019**, *39*, 35–44. [CrossRef]

80. Schallenberg, M.; Burns, C.W. Effects of sediment resuspension on phytoplankton production: Teasing apart the influences of light, nutrients and algal entrainment. *Freshw. Biol.* **2004**, *49*, 143–159. [CrossRef]

81. Lázaro-Vázquez, A.; Castillo, M.M.; Jarquín-Sánchez, A.; Carrillo, A.L.; Capps, K.A. Temporal changes in the hydrology and nutrient concentrations of a large tropical river: Anthropogenic influence in the Lower Grijalva River, Mexico. *River. Res. Appl.* **2018**, *34*, 649–660. [CrossRef]

82. Goñi-Arévalo, J.A.; Hernández-Pérez, O.; Toledo-Gómez, J.L.; Pérez Méndez, M.A. Eutroficación de la laguna de las Ilusiones y un modelo empírico de fósforo. *Universidad y Ciencia* **1991**, *8*, 47–53.

83. Hettiarachchi, M.; Morrison, T.H.; Wickramsinghe, D.; Mapa, R.; De Alwis, A.; McAlpine, C.A. The eco-social transformation of urban wetlands: A case study of Colombo, Sri Lanka. *Landsc. Urban Plan.* **2014**, *132*, 55–68. [CrossRef]

84. Sánchez, A.J.; Florido, R.; Salcedo, M.A.; Ruiz-Carrera, V.; Montalvo-Urgel, H.; Raz-Guzmán, A. Macrofaunistic diversity in *Vallisneria americana* Michx. in a tropical wetland, Southern Gulf of Mexico. In *Ecosystems I.*; Mahamane, A., Ed.; InTech: Rijeka, Croatia, 2012; pp. 1–26; ISBN 978-953-51-5289-7.

85. Lone, P.A.; Bhardwaj, A.K.; Shah, K.W. Macrophytes as powerful natural tools for water quality improvement. *Res. J. Bot.* **2014**, *9*, 24–30. [CrossRef]

86. Thoms, M.C. Floodplain–river ecosystems: Lateral connections and the implications of human interference. *Geomorphology* **2003**, *56*, 335–349. [CrossRef]

87. Biswas, S.S.; Pani, P. Changes in the hydrological regime and channel morphology as the effects of dams and bridges in the Barakar River, India. *Environ. Earth Sci.* **2021**, *80*, 1–18. [CrossRef]

88. Zhang, P.; Zhang, H.; Wang, H.; Hilt, S.; Li, C.; Yu, C.; Zhang, M.; Xu, J. Warming alters juvenile carp effects on macrophytes resulting in a shift to turbid conditions in freshwater mesocosms. *J. Appl. Ecol.* **2022**, *59*, 165–175. [CrossRef]

89. Weigelhofer, G.; Preiner, S.; Fun, A.; Bondar-Kunze, E.; Hein, T. The hydrochemical response of small and shallow floodplain water bodies to temporary surface water connections with the main river. *Freshw. Biol.* **2015**, *60*, 781–793. [CrossRef]

90. Moorman, M.C.; Augspurger, T.; Stanton, J.D.; Smith, A. Where's the Grass? Disappearing Submerged Aquatic Vegetation and Declining Water Quality in Lake Mattamuskeet. *J. Fish Wildl. Manag.* **2016**, *8*, 401–417. [CrossRef]